High-performance Optical Modulator Based on Electro-optic Polymer Infiltrated Silicon Slot Photonic Crystal Waveguide

[1]Xingyu Zhang*, [2]Amir Hosseini, [3]Jingdong Luo, [3]Alex K.-Y. Jen, and [1]Ray T. Chen*
[1]Microelectronics Research Center, Electrical and Computer Engineering Department, University of Texas at Austin, Austin, TX, 78758, USA
[2]Omega Optics, Inc., Austin, TX 78759, USA
[3]Department of Materials Science and Engineering, University of Washington, Seattle, Washington 98195, USA
**Corresponding author: xzhang@utexas.edu, raychen@uts.cc.utexas.edu*

Abstract: We demonstrate a low-dispersion, sub-volt, and compact optical modulator based on electro-optic polymer infiltrated slot photonic crystal waveguide. $V_\pi \times L = 0.291 \pm 0.006$ V×mm and effective in-device r_{33}=1190pm/V over 8nm optical bandwidth are measured.
OCIS codes: (230.4110) Modulators; (130.5296) Photonic crystal waveguides; (200.4650) Optical interconnects; (250.2080) Polymer active devices

Electro-optic (EO) polymer modulators in optical links are promising for low power consumption due to the large EO coefficient of active polymer [1]. In addition to conventional all-polymer devices, the combination of silicon photonics and EO polymer have shown to enable compact and high performance integrated optical modulators [2]. Utilizing slow light effect, photonic crystal waveguides (PCWs) refilled with EO polymers can further reduce the device size [3]. The fabrication process of these devices involves the poling of the EO polymer at an elevated temperature. Unfortunately, the leakage current due to the charge injection through silicon/polymer interface significantly reduces the poling efficiency in narrow slot waveguides (slot width, S_w<200nm). Among the abovementioned structure, the slot PCW can support optical mode for S_w as large as 320nm [4]. Such a wide slot was shown to reduce the leakage current by two orders of magnitude resulting in 5x improvement in the in-device r_{33} compared to a slot PCW with S_w=75nm [4], while high optical confinement and low optical loss in the slot is still achieved with the help of efficient mode converters [5]. One problem remaining among PCW modulators is their narrow operating optical bandwidth of <1nm, because of the high group velocity dispersion in the slow-light optical spectrum range. To broaden the optical bandwidth of PCW modulators, lattice shifted PCWs are developed to provide low-dispersion slow light (constant group velocity, v_g) [6].

In this letter we report a low-dispersion, sub-volt MZI modulator based on band-engineered slot PCW refilled with EO polymer. The EO polymer used here is SEO125 from Soluxra, LLC, with EO coefficient (r_{33}) of 125pm/V. Using a band-engineered EO polymer refilled slot PCW with S_w=320nm, we demonstrate a slow-light enhanced effective in-device r_{33} of 1190pm/V and $V_\pi \times L$ of 0.291 ± 0.006 V×mm over 8nm optical spectrum range. Excluding the slow-light effect, we estimate in-device material r_{33} of 89pm/V for SEO125 in the slot that show 51% improvement compared to the results (59pm/V) in [4]. To the best of our knowledge, our modulator performance is a new record among silicon/polymer hybrid modulators, due to its largest effective in-device r_{33}, the smallest $V_\pi \times L$ and the highest EO polymer poling efficiency.

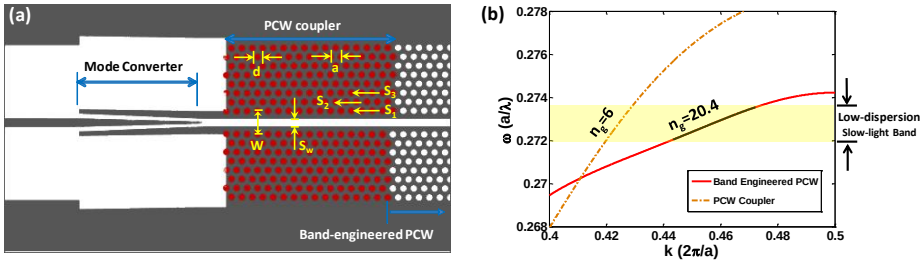

Fig. 1. (a) Layout of the PCW coupler (mode converter + PCW coupler). The black area corresponds to un-etched silicon. (b) Band diagram of the engineered slow-light PCW and the PCW coupler.

A schematic of the device on SOI (Si thickness=250nm, oxide thickness=3μm) is shown in Fig. 1 (a). The input and output strip waveguides are connected to the device using a strip- to slot-waveguide mode converter. PCW couplers consisting of a fast-light section [7] connect the mode converters to a 300μm-long slow-light PCW section. The slow-light PCW section is band-engineered by lateral shifting of the first three rows on the two sides of the slot [indicated by s_1, s_2, s_3 in Fig. 1 (a)] and by varying the center-to-center distance between two rows adjacent to the

slot [W in Fig. 1 (a)]. For lattice constant, a=425nm, it is found that with a hole diameter d=300nm, s_1=0, s_2=-85nm, s_3=85nm, S_w=320nm, and W=1.54(√3)a, we can achieve an average group index (n_g=c/v_g) of 20.4 (±10%) over 8.2nm optical bandwidth. The PCW step coupler [a=425nm, d=300nm, s_1=0, s_2=0, s_3=0, S_w=320nm, W=1.45(√3)a] consists of 16 periods and is designed for low n_g=6 over the same wavelength range. The band diagrams of the slow-light and fast-light PCWs are shown in Fig. 1 (b).

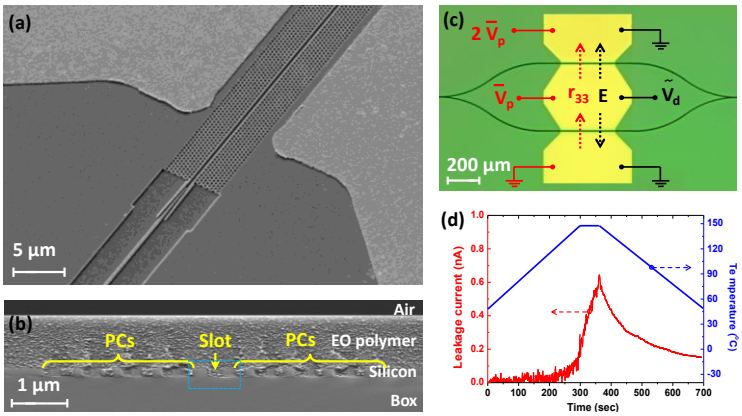

Fig. 2. (a) SEM image of one arm of the fabricated silicon slot PCW modulator (tilted view). (b) SEM image of the EO polymer refilled silicon slot PCW (cross-sectional view). PCs: photonic crystals. (c) Optical microscope image of the fabricated slot PCW MZI modulator (top view). The red colored circuit connection indicates push-pull poling configuration and induced r_{33} direction, and the black colored circuit connection indicates the modulation configuration. V_p: poling voltage, V_d: diving voltage. (d) Temperature-dependent leakage current in EO polymer poling process.

The fabrication procedure starts with an SOI wafer with 250nm-thick top silicon. All the photonic circuitries are fabricated using e-beam lithography and RIE, while the gold electrodes are patterned by photolithography and lift-off process. The EO polymer is infiltrated into the slot PCW by spincoating. The silicon PCW regions including holes and the slot are fully covered by EO polymer, as shown in the SEM image in Fig. 1 (c). A microscope image of the fabricated MZI is shown in Fig. 1 (d). Next, the sample is poled by an electric field of 100V/μm in a push-pull configuration at the glass transition temperature (T_g=145 ℃) of the EO polymer [8]. The monitored leakage current depending on hot plate temperature is shown in Fig. 2(a). It can be seen that the leakage current density remains below 1.4×10^{-6}A/m^2 [=103μA/(300μm×250nm)]. For comparison, the leakage current density in the SEO125 data sheet is 2.36×10^{-6}A/m^2 measured in a thin film configuration. This test result shows that the 320nm-wide slot dramatically reduces the leakage current that is known to be detrimental to the poling efficiency [9].

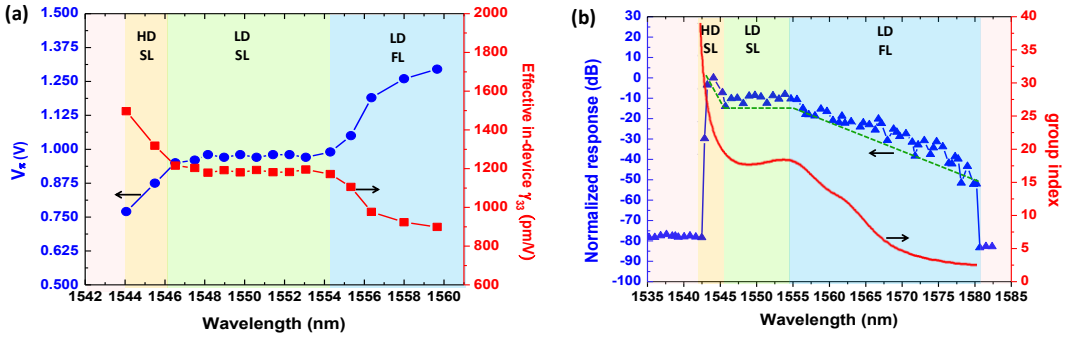

Fig. 3. (a) Measured V_π and corresponding calculated effective in-device r_{33} v.s. wavelength (at 100KHz). HD SL: high-dispersion slow-light; LD SL: low-dispersion slow-light; LD FL: low-dispersion fast-light. (b) Normalized device response v.s. wavelength (at 100KHz). The green dashed line indicates the trend of the response change over different wavelength. The simulated n_g v.s. wavelength is also overlaid.

For modulation test, TE-polarized light from a tunable laser source (1550nm, 2.5mW) is coupled into and out of the device through grating couplers. RF signals are applied to the electrodes as shown in Fig. 1 (d). The modulator is biased at the 3dB point and driven by a 100KHz triangular RF wave with a peak-to-peak voltage of 1.4V. The modulated output optical signal is sent to a photodetector and then displayed on a digital oscilloscope. The V_π of the modulator is measured to be 0.973V, by observing the transfer function of the over-modulated optical signal and the input RF signal on the oscilloscope [10]. The effective in-device r_{33} is then calculated to be

$$r_{33-\text{effective}} = \frac{\lambda S_w}{n^3 V_\pi \sigma L} = 1190\text{pm/V} \quad (1)$$

where, λ=1550nm, S_w=320nm, n=1.63, L=300μm, σ=0.33 (confinement factor in the slot) calculated by simulation. This extraordinarily high r_{33} value confirms the combined enhancing effects of slow light and an improved poling efficiency. This modulator also achieves very high modulation efficiency with V_π×L=0.973V×300μm=0.292V×mm. We also estimate the actual in-device r_{33} excluding the slow-light effect using [6]

$$L = \frac{\lambda}{2\sigma n_g}\left(\frac{n}{\Delta n}\right) \quad (2)$$

where, $\Delta n = n^3 r_{33} V_\pi / (2S_w)$. The estimated in-device r_{33} is 89pm/V which is the highest poling efficiency demonstrated in a slot waveguide, to the best of our knowledge.

To demonstrate the low dispersion, the optical wavelength is tuned over a wide optical bandwidth from 1544nm to 1560nm while all other testing conditions are fixed. The V_π measured at different wavelength, as well as the corresponding calculated effective in-device r_{33}, is plotted in Fig. 2 (b). It can be seen that the V_π is nearly constant, which is 0.97±0.02V, over optical spectrum range of 8nm (low-dispersion slow-light region: from 1546.5nm to 1554.5nm), corresponding to the effective in-device r_{33} of 1190pm/V and V_π×L of 0.291 ± 0.006V×mm. Furthermore, a small signal modulation test is done at V_{pp}<1V over a range of wavelength from 1535nm to 1582nm, while all other testing conditions remain the same. The wavelength dependence of the normalized optical response is plotted in Fig. 2 (c). It can be seen that the defect-guided mode of slot PCW occurs from 1543nm to 1580nm. A maximum response occurs at the high-dispersion slow-light region (1543nm-1546.5nm), because of the largest n_g in this region. The response is almost flat in the low-dispersion slow-light region (1546.5nm-1554.5nm), because the slot PCW is band-engineered with a nearly constant n_g in this wavelength range. As the optical signal is tuned to longer wavelength (low-dispersion fast-light region: 1554.5nm-1580nm), the device response becomes smaller due to decreasing n_g. Details are discussed in [11]. In addition, by selectively doping the silicon PCW to reduce RC constant [12], we have achieved the modulation up to 10 GHz [13]. Due to page limits, further results about modulation bandwidth will be presented in the conference. Our future work includes expanding the research work to a sensitive and broadband integrated photonic electromagnetic field sensor [14,15] using a similar PCW structure.

Reference

[1] Y. Shi, C. Zhang, H. Zhang, J. H. Bechtel, L. R. Dalton, B. H. Robinson, and W. H. Steier, "Low (sub-1-volt) halfwave voltage polymeric electro-optic modulators achieved by controlling chromophore shape," *Science*, vol. 288, pp. 119-122, 2000.

[2] X. Zhang, A. Hosseini, X. Lin, H. Subbaraman, and R. T. Chen, "Polymer-based Hybrid Integrated Photonic Devices for Silicon On-chip Modulation and Board-level Optical Interconnects," *IEEE Journal of Selected Topics in Quantum Electronics*, vol. 16, pp. 3401115-3401115, 2013.

[3] J. M. Brosi, C. Koos, L. C. Andreani, M. Waldow, J. Leuthold, and W. Freude, "High-speed low-voltage electro-optic modulator with a polymer-infiltrated silicon photonic crystal waveguide," *Optics Express*, vol. 16, pp. 4177-4191, 2008.

[4] X. Wang, C.-Y. Lin, S. Chakravarty, J. Luo, A. K.-Y. Jen, and R. T. Chen, "Effective in-device r< sub> 33</sub> of 735 pm/V on electro-optic polymer infiltrated silicon photonic crystal slot waveguides," *Optics letters*, vol. 36, pp. 882-884, 2011.

[5] X. Zhang, H. Subbaraman, A. Hosseini, and R. T. Chen, "Optimization of Highly Efficient Mode Converter for Coupling Light into Wide slot Photonic Crystal Waveguide" (Under review)

[6] A. Hosseini, X. C. Xu, H. Subbaraman, C. Y. Lin, S. Rahimi, and R. T. Chen, "Large optical spectral range dispersion engineered silicon-based photonic crystal waveguide modulator," *Optics Express*, vol. 20, pp. 12318-12325, May 21 2012.

[7] A. Hosseini, X. Xu, D. N. Kwong, H. Subbaraman, W. Jiang, and R. T. Chen, "On the role of evanescent modes and group index tapering in slow light photonic crystal waveguide coupling efficiency," *Applied Physics Letters*, vol. 98, pp. 031107-031107-3, 2011.

[8] X. Lin, T. Ling, H. Subbaraman, X. Zhang, K. Byun, L. J. Guo, and R. T. Chen, "Ultraviolet imprinting and aligned ink-jet printing for multilayer patterning of electro-optic polymer modulators," *Optics letters*, vol. 38, pp. 1597-1599, 2013.

[9] X. Zhang, B. Lee, C.-y. Lin, A. X. Wang, A. Hosseini, and R. T. Chen, "Highly Linear Broadband Optical Modulator Based on Electro-Optic Polymer," *Photonics Journal, IEEE*, vol. 4, pp. 2214-2228, 2012.

[10] X. Zhang, A. Hosseini, C.-y. Lin, J. Luo, A. K. Jen, and R. T. Chen, "Demonstration of Effective In-device r33 over 1000 pmV in Electro-optic Polymer Refilled Silicon Slot Photonic Crystal Waveguide Modulator," in *CLEO: Science and Innovations*, 2013.

[11] X. Zhang, A. Hosseini, S. Chakravarty, J. Luo, A. K.-Y. Jen, and R. T. Chen, "Wide optical spectrum range, subvolt, compact modulator based on an electro-optic polymer refilled silicon slot photonic crystal waveguide," *Optics letters*, vol. 38, pp. 4931-4934, 2013.

[12] X. Zhang, A. Hosseini, X. Xu, S. Wang, Q. Zhan, Y. Zou, S. Chakravarty, and R. T. Chen, "Electric field sensor based on electro-optic polymer refilled silicon slot photonic crystal waveguide coupled with bowtie antenna," in *SPIE OPTO*, 2013, pp. 862418-862418-8.

[13] X. Zhang, A. Hosseini, H. Subbaraman, J. Luo, A. K.-Y Jen, and R. T. Chen, "40GHz, 0.16pJ/bit, Compact Optical Modualtor Based on Electro-optic Polymer Infiltrated Silicon Slot Photonic Crystal Waveguide," (In preparation)

[14] C.-Y. Lin, A. X. Wang, B. S. Lee, X. Zhang, and R. T. Chen, "High dynamic range electric field sensor for electromagnetic pulse detection," *Opt. Exp*, vol. 19, pp. 17372-17377, 2011.

[15] X. Zhang, A. Hosseini, H. Subbaraman, S.Wang, Q. Zhan, J. Luo, A. K.-Y Jen, and R. T. Chen, "Integrated Photonic Electromagnetic Field Sensor Based on Broadband Bowtie Antenna Coupled Silicon Organic Hybrid Modulator," Journal of Lightware Technology (Accepted)